Catalytic Kinetics of Different Types of Surface Atoms on Shaped Pd Nanocrystals

Tao Chen, Sheng Chen, Yuwei Zhang, Yifeng Qi, Yuzhou Zhao, Weilin Xu,* and Jie Zeng*

Abstract: *To understand the catalytic properties or roles of different types of surface atoms on metal nanocatalysts, the catalytic kinetics and dynamics of the different types of surface atoms (plane and edge) were revealed for the first time by a statistical quantitative deconvolution of observables obtained from traditional single-molecule nanocatalysis of Pd nanocrystals. It was found that the edge and plane of Pd nanocubes show similar size-dependent product formation processes, but inverse product dissociation processes. This work helps push the traditional single-molecule nanocatalysis method towards the sub-particle level.*

*H*eterogeneous nanocatalysis has attracted considerable attention over the past decades because of its broad applications during chemical manufacturing processes.[1] However, study is often hampered by the difficulty of identifying the properties or roles of different types of surface atoms, such as the plane, edge, or corner atoms on a single nanoparticle surface.[2–4] To elucidate this problem, various experiments and computations have been conducted,[2,4–10] but it is still difficult to clarify the quantitative contribution of different types of surface atoms to the total catalytic reactivity of a single nanoparticle. In recent years, single-molecule fluorescence microscopy (SMFM) has been used to investigate the kinetic and dynamic behaviors of the whole single nanoparticles in real time with single-turnover resolution.[11–19] Furthermore, the activity of different parts of an individual nanocatalyst (from a few hundred nanometers to microns in size) was visualized approximately using super-

resolution fluorescence microscopy.[20–22] However, owing to the limitation of spatial resolution and the vague partition of corner, edge, or plane on individual nanocatalysts, the catalytic kinetic and dynamic study of different types of surface atoms cannot be studied quantitatively with SMFM.

In this work, based on well-defined palladium (Pd) nanocubes and rational physical models, by a statistical quantitative deconvolution of observables obtained from traditional single-molecule nanocatalysis of Pd nanocrystals, the catalytic kinetics and dynamics of the different types of surface atoms (plane and edge) were studied quantitatively for the first time. This work pushes traditional SMFM a step forward to sub-particle level.[18]

Here, the face-centered cubic (fcc) Pd nanocubes with uniform sizes were synthesized according to previous methods (Supporting Information).[23–24] Figures 1a–c and S1a,b
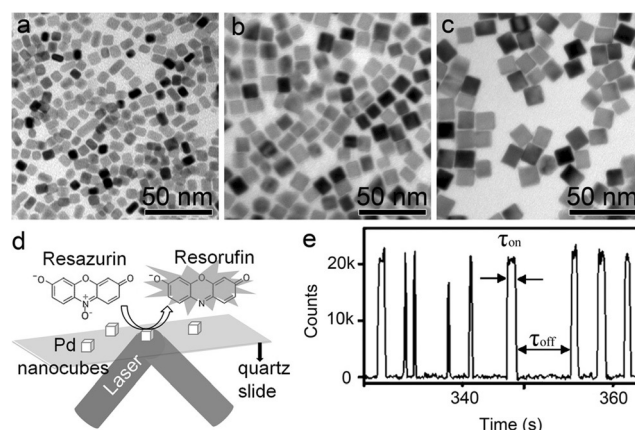

Figure 1. Single-molecule nanocatalysis. a–c) Typical TEM images of three sets of Pd nanocubes with size a) 7.0 nm, b) 11.4 nm, and c) 15.2 nm. d) Experimental setup for single-molecule catalysis based on Pd-catalyzed reduction of Resazurin to fluorescent Resorufin by H_2 using total internal reflection fluorescence microscopy. e) Representative fluorescence intensity vs. time of a single 15.2 nm Pd nanoparticle under catalysis with 1 nм Resazurin under saturated H_2 at an imaging rate of 100 ms per frame.

[*] T. Chen, Y. Zhang, Prof. Dr. W. Xu
State Key Laboratory of Electroanalytical Chemistry and
Jilin Province Key Laboratory of Low Carbon Chemical Power
Changchun Institute of Applied Chemistry
Chinese Academy of Science
5625 Renmin Street, Changchun 130022 (P.R. China)
E-mail: weilinxu@ciac.ac.cn

S. Chen, Y. Qi, Y. Zhao, Prof. Dr. J. Zeng
Hefei National Laboratory for Physical Sciences at the Microscale
and
Collaborative Innovation Center of Suzhou Nano Science and
Technology
Center of Advanced Nanocatalysis (CAN-USTC) and
Department of Chemical Physics
University of Science and Technology of China
Hefei, Anhui 230026 (P. R. China)
E-mail: zengj@ustc.edu.cn

T. Chen
University of Chinese Academy of Sciences
Beijing 100049 (P. R. China)

Supporting information for this article is available on the WWW
under http://dx.doi.org/10.1002/anie.201509165.

show typical transmission electron microscope (TEM) images of five sets of Pd nanocubes in different sizes. The fcc Pd nanocube is mainly enclosed by {100} facets, which was confirmed by Figure S1c–e.[25] The corresponding size and shape distributions are shown in Figures S2 and S3, where the five sets of Pd nanocubes were, on average, 5.2, 7.0, 11.4, 15.2, and 22.2 nm in edge length, respectively. Single-molecule nanocatalysis was performed based on the hydrogenation of Resazurin catalyzed by Pd nanocubes (Figure 1d; Supporting

Information, Figures S4 and S5). The product molecule of this reaction is the fluorescent Resorufin that can be individually detected by single nanoparticle surface with SMFM.[18] To image this catalytic process, we immobilized the diluted nanocubes on a quartz slide in a microfluidic reactor cell and supplied the reactants in a constant flow (Figure 1 d). Under a total internal reflection fluorescence microscope, each product molecule of Resorufin was excited by a 532 nm laser and the fluorescence was detected. Figure 1 e shows a part of a typical single-molecule fluorescence trajectory from a single 15.2 nm Pd nanocube. It contains intensity bursts with consistent height, and each burst corresponds to one product molecule, that is, one catalytic turnover, and the duration (τ_{on}) of each burst reports the time each Resorufin molecule spends before it dissociates and then diffuses away from the nanocatalyst surface. The duration (τ_{off}) is the waiting time before the formation of each Resorufin molecule.[18] Control experiments exclude the possible effect of residual surfactants (Figure S6 and S7), and further confirm that the observed signals originated from the reduction of Resazurin by H_2 catalyzed by Pd: No digital fluorescence bursts are observed in the absence of either Pd nanocube, H_2, or Resazurin.

Statistically, $\langle\tau_{off}\rangle^{-1}$ and $\langle\tau_{on}\rangle^{-1}$ (where $\langle\rangle$ denotes averaging) represent the time-averaged single-particle rates of product formation and product dissociation, respectively. When averaged over the turnover trajectories from many Pd nanoparticles with the same size, $\langle\tau_{off}\rangle^{-1}$ and $\langle\tau_{on}\rangle^{-1}$ are expectedly dependent on the Resazurin concentration (Figure 2 a,b).[18,26] Interestingly, the product formation rates ($\langle\tau_{off}\rangle^{-1}$) for these five sets of nanoparticles (Figure 2 a) all increase with substrate concentration first, then decrease after a maximum, indicating a two-site Langmuir–Hinshelwood mechanism of the catalytic kinetics on these Pd nanocatalysts.[7,13] Figure 2 b shows that the product dissociation rates ($\langle\tau_{on}\rangle^{-1}$) on three small (5.2 nm, 7.0 nm, and 11.4 nm) nanoparticles decrease with substrate concentration (Figure 2 b), while the rates increase with substrate concentration on large (15.2 nm and 22.2 nm) Pd nanoparticles, indicating that two different product dissociation pathways, direct and substrate-associated indirect pathways, coexist in this catalytic system.[18] Figure 2 c shows the total mechanism for a complete turnover based on the two-site Langmuir–Hinshelwood mechanism for the product formation process.[18] Based on statistical single-molecule analysis (Supporting Information), we obtained the product formation rate:

$$\langle\tau_{off}\rangle^{-1} = \frac{\gamma_{eff} a_A[A] a_B[B]}{(1 + a_A[A] + a_B[B])^2} \qquad (1)$$

and the product dissociation rate:

$$\langle\tau_{on}\rangle^{-1} = \frac{\gamma_2 G[B] + \gamma_3}{1 + G[B]} \qquad (2)$$

where [A] and [B] are the H_2 and Resazurin concentrations, respectively; γ_{eff} is the rate constant representing the intrinsic reactivity per nanoparticle for the catalytic conversion reaction; a_A and a_B are the adsorption constants of H_2 and
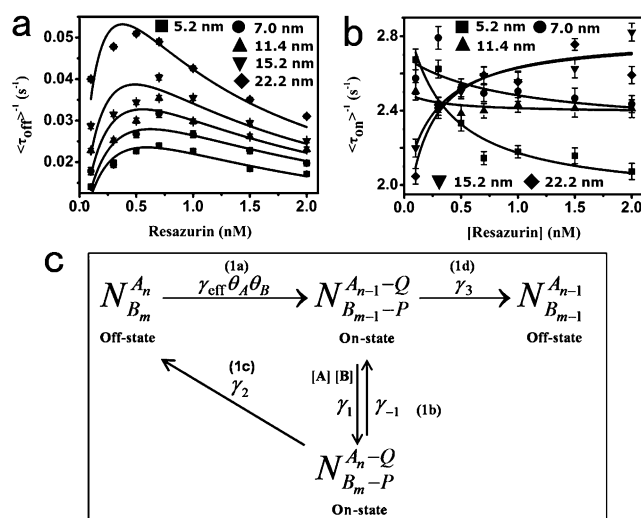

Figure 2. a,b) Resazurin concentration dependence of product formation rates ($\langle\tau_{off}\rangle^{-1}$) and product dissociation rates ($\langle\tau_{on}\rangle^{-1}$) on 5.2 nm, 7.0 nm, 11.4 nm, 15.2 nm, and 22.2 nm Pd nanocubes. Each data point is averaged over the turnover trajectories of > 50 nanoparticles. Error bar = s.e.m. Solid lines are fitted with Equations (1) and (2); the fitting results are summarized in Table S1. c) Diagram of the kinetic mechanism for a whole catalytic turnover. N represents one Pd nanoparticle; A, B, Q, and P represent hydrogen, Resazurin, water, and Resorufin molecules, respectively; n, m, the number of H_2 and Resazurin molecules adsorbed on one nanoparticle surface at equilibrium; γ_{eff} the effective rate constant for the product formation step; γ_i the rate constants for different product dissociation steps; θ_A, θ_B, the fraction of the surface occupied by hydrogen and Resazurin.

Resazurin; γ_2 and γ_3 are the rate constants for the indirect and direct dissociation of product; G ($= [A]\gamma_1/(\gamma_{-1} + \gamma_2)$) is a complex parameter without clear physical meaning but related to both the substrate adsorption (γ_1)/desorption (γ_{-1}) and the indirect product dissociation process (γ_2).

For a Pd nanocube enclosed by {100} facets, apparently, the total surface atoms can be divided into three main types. The first type is the atoms on plane noted as p; the second is the atoms at edge noted as e; and the third is the atoms on corner noted as c. For Pd nanocubes with size larger than 5 nm, the portion of corner atoms on the whole surface of a single Pd nanocube is too small to be reliably differentiated.[7,27] In this case, the corner atoms were simply neglected and only two types (p and e) of surface atoms were considered. Based on the statistics of surface atoms,[27,28] for *fcc* nanocrystals, the numbers (N_{plane} and N_{edge}, both of them are dimensionless) of different types of surface atoms on a single nanocrystal with a particular size and shape can be determined (Figure S8). Therefore, the fractions ($x_p = N_{plane}/N_S$, $x_e = N_{edge}/N_S$) of different types of surface atoms can be derived by a statistical calculation of surface atoms for *fcc* nanocrystals (the number of surface atoms per particle: $N_S = 12 m^2 - 12 m - 4$, where m is the number of atoms on an equivalent edge of a nanocube; see the Supporting Information). Table S2 summarizes the statistical data for Pd nanocubes in different sizes used in this work.

Based on the data shown in Table S2, we decompose the obtained values of $\langle\tau_{off}\rangle^{-1}$ and $\langle\tau_{on}\rangle^{-1}$ shown in Figure 2 a,b

into two parts, respectively corresponding to the two types of surface atoms (*p* and *e*) mentioned above. For the decomposition of $\langle\tau_{\text{off}}\rangle^{-1}$, with the assumption that the observed activity depends linearly on the fraction (x_i) of each type of surface atoms and their specific activity,[7] the following model (Off-Model) is proposed to evaluate the contributions of plane and edge atoms to the total product formation rate per particle(Off-Model, Supporting Information):

$$\langle\tau_{\text{off}}\rangle^{-1} = \langle\tau_{\text{off,plane}*}\rangle^{-1}N_{\text{plane}}x_p + \langle\tau_{\text{off,edge}*}\rangle^{-1}N_{\text{edge}}x_e \tag{3}$$

Off-Model means the product formation rate ($\langle\tau_{\text{off}}\rangle^{-1}$) averaged from a whole particle contains two terms. One term ($\langle\tau_{\text{off,plane}*}\rangle^{-1}N_{\text{plane}}x_p$) is the real contribution from all the plane atoms (N_{plane}) on this particle surface; the other ($\langle\tau_{\text{off,edge}*}\rangle^{-1}N_{edge}x_e$) is the real contribution from all the edge atoms (N_{edge}) on this particle surface. For each term, $\langle\tau_{\text{off,plane}*}\rangle^{-1}$ or $\langle\tau_{\text{off,edge}*}\rangle^{-1}$ is defined as the apparent average product formation rate per plane atom or edge atom, and was assumed and subsequently confirmed to be independent of the particle size (Figure S9) because the size effect has been reflected by N_{plane} or N_{edge}. By contrast, the term $\langle\tau_{\text{off,plane}*}\rangle^{-1}N_{\text{plane}}$ or $\langle\tau_{\text{off,edge}*}\rangle^{-1}N_{\text{edge}}$ represents the product formation rate from all the plane or edge atoms and is particle-size-dependent.

As for the product dissociation rate ($\langle\tau_{\text{on}}\rangle^{-1}$) per particle, similarly,based on the assumption mentioned above,[7] the On-Model is proposed to decompose $\langle\tau_{\text{on}}\rangle^{-1}$:

$$\langle\tau_{\text{on}}\rangle^{-1} = \langle\tau_{\text{on,plane}*}\rangle^{-1}x_p + \langle\tau_{\text{on,edge}*}\rangle^{-1}x_e \tag{4}$$

On-model means that the product dissociation rate $\langle\tau_{\text{on}}\rangle^{-1}$ averaged from a whole single nanoparticle contains two contributions: one ($\langle\tau_{\text{on,plane}*}\rangle^{-1}x_p$) is the real contribution from all plane atoms on this nanoparticle, the other ($\langle\tau_{\text{on,edge}*}\rangle^{-1}x_e$) is the real contribution from all edge atoms on this nanoparticle. Since the dissociation of an individual product molecule is only related to the property of the individual (*p* or *e*) site where the individual product molecule adsorbs and then approximately independent of the total number of surface *p* or *e* sites, the terms of $\langle\tau_{\text{on,plane}*}\rangle^{-1}$ and $\langle\tau_{\text{on,edge}*}\rangle^{-1}$ are the apparent average product dissociation rates per plane atom and per edge atom, respectively, and were assumed and subsequently confirmed to be independent of nanoparticle size (Figure S10).

Since the values of $\langle\tau_{\text{off}}\rangle^{-1}$, $\langle\tau_{\text{on}}\rangle^{-1}$, N_{plane}, x_p, N_{edge}, and x_e have been obtained as shown in Figure 2 and Table S2, the Off-Model for $\langle\tau_{\text{off}}\rangle^{-1}$ and On-Model for $\langle\tau_{\text{on}}\rangle^{-1}$ can be applied simultaneously to any two (AB, AC, BC, AD, BD, CD, AE, BE, CE, and DE) of the five (A: 5.2 nm; B: 7.0 nm; C: 11.4 nm; D: 15.2 nm; E: 22.2 nm) size-different Pd-nanocubes to extract the values of $\langle\tau_{\text{off,plane}*}\rangle^{-1}$ and $\langle\tau_{\text{off,edge}*}\rangle^{-1}$, $\langle\tau_{\text{on,plane}*}\rangle^{-1}$ and $\langle\tau_{\text{on,edge}*}\rangle^{-1}$ by solving two two-variable linear equations, respectively, at various substrate concentrations (Figures S9 and S10). Based on the values of N_{plane} and N_{edge} on size-different Pd nanoparticles, we further obtained the product formation rate of all the plane atoms on one nanocube: $\langle\tau_{\text{off,plane}}\rangle^{-1} = \langle\tau_{\text{off,plane}*}\rangle^{-1}N_{\text{plane}}$, and the product formation rate of all the edge atoms on one nanocube: $\langle\tau_{\text{off,edge}}\rangle^{-1} =$
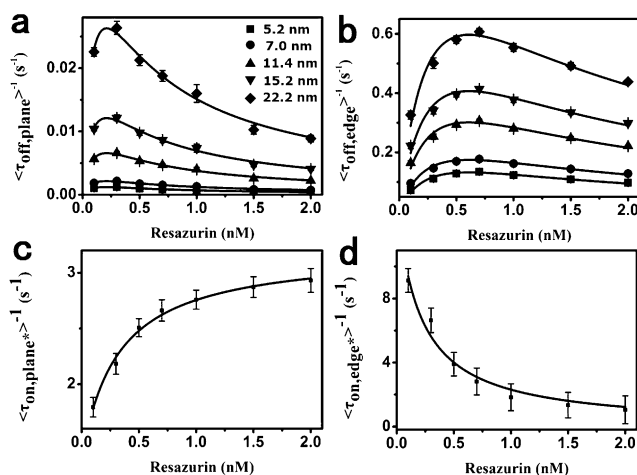
Figure 3. a,b) The substrate Resazurin concentration dependence of product formation rates ($\langle\tau_{\text{off,plane}}\rangle^{-1}$) on a) plane sites, and b) edge sites ($\langle\tau_{\text{off,edge}}\rangle^{-1}$) on five sets of size-different Pd nanocubes; c,d) The Resazurin concentration dependence of product dissociation rates averaged on one plane site c) $\langle\tau_{\text{on,plane}*}\rangle^{-1}$, and edge site d) $\langle\tau_{\text{on,edge}*}\rangle^{-1}$. The hydrogen concentration was fixed at 0.8 mM. Solid lines are the fits with Equation (5–8). All fitting values are summarized in Table S3 and Table S5. Error bars = s.e.m.

$\langle\tau_{\text{off,edge}*}\rangle^{-1}N_{\text{edge}}$. As shown in Figure 3a,b, for all of the nanocubes with five different sizes, both $\langle\tau_{\text{off,plane}}\rangle^{-1}$ and $\langle\tau_{\text{off,edge}}\rangle^{-1}$, the product formation rates of all of the plane atoms and edge atoms on one nanocube increase with Resazurin concentration first, then decrease inversely after a maximum, similar to that shown in Figure 2a, indicating a two-site Langmuir–Hinshelwood mechanism of the catalytic kinetics on both plane and edge of the nanocube. As for the dissociation of individual product molecules from different types of surface atoms, Figure 3c shows that the product dissociation rate on plane atoms ($\langle\tau_{\text{on,plane}*}\rangle^{-1}$) increases with substrate concentration, while the product dissociation rate on edge atoms ($\langle\tau_{\text{on,edge}*}\rangle^{-1}$) decreases inversely with substrate concentration (Figure 3d). All of these facts indicate the coexistence of both direct and indirect dissociation pathways on both plane and edge sites.[18]

According to the total catalytic mechanism shown in Figure 2c and the Equations (1–2), the kinetic equations for the product formation rate of all the plane atoms or all the edge atoms, and the average product dissociation rate on a plane or edge atom (site) of the nanocube can be deduced as following:

$$\langle\tau_{\text{off,plane}}\rangle^{-1} = \frac{\gamma_{\text{eff,p}}\,a_{\text{A,p}}[\text{A}]\,a_{\text{B,p}}[\text{B}]}{(1 + a_{\text{A,p}}[\text{A}] + a_{\text{B,p}}[\text{B}])^2} \tag{5}$$

$$\langle\tau_{\text{off,edge}}\rangle^{-1} = \frac{\gamma_{\text{eff,e}}\,a_{\text{A,e}}[\text{A}]\,a_{\text{B,e}}[\text{B}]}{(1 + a_{\text{A,e}}[\text{A}] + a_{\text{B,e}}[\text{B}])^2} \tag{6}$$

$$\langle\tau_{\text{on,plane}*}\rangle^{-1} = \frac{\gamma_{2,\text{p}}\,G_{\text{p}}[\text{B}] + \gamma_{3,\text{p}}}{1 + G_{\text{p}}[\text{B}]} \tag{7}$$

$$\langle\tau_{\text{on,edge}*}\rangle^{-1} = \frac{\gamma_{2,\text{e}}\,G_{\text{e}}[\text{B}] + \gamma_{3,\text{e}}}{1 + G_{\text{e}}[\text{B}]} \tag{8}$$

where $\gamma_{\text{eff},i}$ is the effective rate constant representing the intrinsic reactivity of all the plane (p) or edge (e) atoms on one nanoparticle for the catalytic conversion reaction; $a_{A,i}$ and $a_{B,i}$ the adsorption constants for H_2 and Resazurin on plane or edge atoms; $\gamma_{2,i}$ and $\gamma_{3,i}$ the rate constants for the indirect and direct dissociation of product on plane or edge site; G_i ($=\gamma_{1,i}/(\gamma_{-1,i}+\gamma_{2,i})$) is a complex parameter without clear physical meaning.

By fitting the data shown in Figure 3a,b with the above Equations (5–6) with a fixed hydrogen concentration, [A], we can obtain the kinetic parameters for the product formation process on different types (p and e) of surface atoms on individual nanocubes, as shown in Table S3. It shows that $\gamma_{\text{eff},i}$, the effective rate constants ($\gamma_{\text{eff},p}$ and $\gamma_{\text{eff},e}$), representing the intrinsic reactivity of all the plane (p) and edge (e) atoms on one nanoparticle, all increase with the size of nanocubes. The reason is that these effective rate constants ($\gamma_{\text{eff},i}$) contain the contribution of the total numbers (N_i) of plane or edge active sites on one nanoparticle (Supporting Information), and these numbers of active sites is proportional to the size of the nanocubes. The values of $\gamma_{\text{eff},e}$ for all the five size-different Pd nanocubes are approximately two-magnitude larger than those of $\gamma_{\text{eff},p}$, indicating two important facts: i) the intrinsic activity per edge active site (γ_e) is much higher than that per plane site (γ_p); ii) the edge sites contribute much more than the plane sites to the total activity of a single nanoparticle, as can be seen from curves shown in the Figure 3a,b. This fact further confirms a well-known site-specific selectivity or activity of different types of active sites.[2,8] As for the hydrogen adsorption constant (a_A) on the surface Pd atoms, Table S3 shows that this constant is almost independent of the nanoparticle size and the type (p or e) of Pd atoms on surface, which probably could be attributed to the spontaneous fast dissociation of H_2 molecules into atomic hydrogen atoms or protons upon adsorption on Pd nanoparticles.[29] As for the adsorption constant (a_B) of Resazurin on the same type of surface atoms (p or e), its value is also insensitive to the size of Pd nanoparticles, probably owing to the fact that the individual adsorption of molecules is only related to the microenvironment of the adsorption site composed of a few atoms. Interestingly, as shown in Table S3, the value of $a_{B,p}$ is three times that of $a_{B,e}$ on the same Pd nanocubes, indicating that a_B is sensitive to the types of surface atoms. The reason why $a_{B,p}$ is larger than $a_{B,e}$ may be the large flat π-π structure of Resazurin molecule, which tends to be adsorbed on flat plane site stably rather than the sharp edge site (Table S4). Table S3 also shows, compared with the edge site, that the plane site exhibits stronger adsorption ability ($a_{B,p}$) but lower catalytic activity ($\gamma_{\text{eff},p}$) to Resazurin. This phenomenon is consistent with previous observations on individual Au nanocatalysts.[30]

Similarly, by fitting the data shown in Figure 3c,d with the above Equations (7–8), we can obtain the kinetic information of the product dissociation process on different types (p and e) of surface atoms on nanocubes (Table S5). The product dissociation from plane sites goes through both the direct and indirect pathways, and the rate constant of the indirect dissociation pathway ($\gamma_{2,p}$) is about three times of that ($\gamma_{3,p}$) of the direct one, indicating that additional substrate (Resazurin) molecules can speed up the product dissociation from

plane sites. While as for the product dissociation from edge site shown in Figure 3d, the dissociation rate decreases with the increase of Resazurin concentration, indicating that additional substrate (Resazurin) molecules can impede the product dissociation from edge sites or $\gamma_{2,e} < \gamma_{3,e}$, just as that shown in Table S5. The obtained value of $\gamma_{2,e}$ (≈ -0.08 s^{-1}) is approximately zero compared with $\gamma_{3,e}$ (≈ 14 s^{-1}; only the non-negative value for this parameter has a reasonable physical meaning), probably indicating that all the product molecules formed on the edge will finally dissociate through the direct pathway.[22] The larger value of G_e compared with G_p probably can be attributed to the fact that $\gamma_{2,e}$ is smaller than $\gamma_{2,p}$. These results show that the different types of surface atoms will lead to different product dissociation kinetics or ability, which can be ascribed to the distinctions of micro-environment around each distinct active site. Theoretically, it is worth to noting here, for a given type of pure surface sites (such as p or e) of a given type of material (such as the Pd nanocubes used here), its product dissociation rate ($\langle\tau_{\text{on,plane*}}\rangle^{-1}$ or $\langle\tau_{\text{on,edge*}}\rangle^{-1}$) per atom should be size-independent, just as that shown in Figure 3c,d and Figure S10. By contrast, for the observed real product dissociation rate ($\langle\tau_{on}\rangle^{-1}$) averaged from a whole single nanoparticle, as shown in Figure 2b, it could be size-dependent owing to a mix of contributions from different types of surface atoms, as shown in Equation (4).

It should be noted, owing to the effects of polydispersed sizes and shapes (Figure S1–S3) as well as the surface defects or restructuring of particles on statistics and orientation of surface atoms, the catalytic kinetics revealed here for different types of surface atoms probably could reflect the properties of such a complicated surface structure.

In summary, based on five sets of Pd nanocubes with different sizes, we revealed the catalytic kinetics and dynamics of different types of surface atoms (plane and edge) by the quantitative deconvolution of observables from traditional single-molecule nanocatalysis, pushing the traditional single-molecule method a step forward. The strategy reported here represents a powerful nanotechnology to study the catalytic properties of different parts or types of surface atoms on a single nanoparticle surface, which can provide insights into the surface properties at the sub-particle level and effectively guide the rational design of functional materials.

[1] G. Bergeret, P. Gallezot, G. Ertl, H. Knözinger, J. Weitkamp, *Handbook of heterogeneous catalysis*, VCH, Weinheim, **1997**.

[2] T. F. Jaramillo, K. P. Jørgensen, J. Bonde, J. H. Nielsen, S. Horch, I. Chorkendorff, *Science* **2007**, *317*, 100–102.

[3] G. A. Somorjai, Y. Li, *Introduction to surface chemistry and catalysis*, Wiley, Hoboken, **2010**.

[4] T. Zambelli, J. Wintterlin, J. Trost, G. Ertl, *Science* **1996**, *273*, 1688–1690.

[5] W. Zhu, et al., *J. Am. Chem. Soc.* **2013**, *135*, 16833–16836.

[6] C. M. Sánchez-Sánchez, J. Solla-Gullón, F. J. Vidal-Iglesias, A. Aldaz, V. Montiel, E. Herrero, *J. Am. Chem. Soc.* **2010**, *132*, 5622–5624.

[7] M. Crespo-Quesada, A. Yarulin, M. Jin, Y. Xia, L. Kiwi-Minsker, *J. Am. Chem. Soc.* **2011**, *133*, 12787–12794.

[8] N. M. Andoy, X. Zhou, E. Choudhary, H. Shen, G. Liu, P. Chen, *J. Am. Chem. Soc.* **2013**, *135*, 1845–1852.

[9] H. Zheng, et al., *Science* **2011**, *333*, 206–209.

[10] S. C. Lai, P. V. Dudin, J. V. Macpherson, P. R. Unwin, *J. Am. Chem. Soc.* **2011**, *133*, 10744–10747.

[11] X. Zhou, W. Xu, G. Liu, D. Panda, P. Chen, *J. Am. Chem. Soc.* **2010**, *132*, 138–146.

[12] G. De Cremer, B. F. Sels, D. E. De Vos, J. Hofkens, M. B. J. Roeffaers, *Chem. Soc. Rev.* **2010**, *39*, 4703–4717.

[13] K. S. Han, G. Liu, X. Zhou, R. E. Medina, P. Chen, *Nano Lett.* **2012**, *12*, 1253–1259.

[14] P. Chen, et al., *Chem. Soc. Rev.* **2014**, *43*, 1107–1117.

[15] S. K. Das, Y. Liu, S. Yeom, D. Y. Kim, C. I. Richards, *Nano Lett.* **2014**, *14*, 620–625.

[16] J. W. Ha, T. P. A. Ruberu, R. Han, B. Dong, J. Vela, N. Fang, *J. Am. Chem. Soc.* **2014**, *136*, 1398–1408.

[17] A. L. Routzahn, P. K. Jain, *Nano Lett.* **2014**, *14*, 987–992.

[18] W. Xu, J. S. Kong, Y. Yeh, P. Chen, *Nat. Mater.* **2008**, *7*, 992–996.

[19] T. Tachikawa, S. Yamashita, T. Majima, *Angew. Chem. Int. Ed.* **2010**, *49*, 432–435; *Angew. Chem.* **2010**, *122*, 442–445.

[20] T. Tachikawa, S. Yamashita, T. Majima, *J. Am. Chem. Soc.* **2011**, *133*, 7197–7204.

[21] X. Zhou, et al., *Nat. Nanotechnol.* **2012**, *7*, 237–241.

[22] M. B. J. Roeffaers, et al., *Angew. Chem. Int. Ed.* **2009**, *48*, 9285–9289; *Angew. Chem.* **2009**, *121*, 9449–9453.

[23] B. Xu, Z. Zhang, X. Wang, *Nanoscale* **2013**, *5*, 4495–4505.

[24] M. Jin, H. Liu, H. Zhang, Z. Xie, J. Liu, Y. Xia, *Nano Res.* **2011**, *4*, 83–91.

[25] G. Collins, M. Schmidt, C. O'Dwyer, J. Holmes, G. P. McGlacken, *Angew. Chem. Int. Ed.* **2014**, *53*, 4142–4146; *Angew. Chem.* **2014**, *126*, 4226–4229.

[26] H. P. Lu, L. Y. Xun, X. S. Xie, *Science* **1998**, *282*, 1877–1882.

[27] R. Van Hardeveld, F. Hartog, *Surf. Sci.* **1969**, *15*, 189–230.

[28] G. C. Bond, *Chem. Soc. Rev.* **1991**, *20*, 441–475.

[29] T. Mitsui, M. K. Rose, E. Fomin, D. F. Ogletree, M. Salmeron, *Nature* **2003**, *422*, 705–707.

[30] W. Xu, J. S. Kong, P. Chen, *Phys. Chem. Chem. Phys.* **2009**, *11*, 2767–2778.